THREE DIMENSIONAL PHOTOELASTIC INVESTIGATIONS ON THICK RECTANGULAR PLATES

by

V.K. Sebastian

Civil Engineering Department
University of Nigeria, Nsukka.
(Manuscript received October 1980)

ABSTRACT
Thick rectangular plates are investigated by means of three-dimensional photoelasticity using the stress-freezing technique. Plate with two opposite edges simply supported and the other two edges free subjected to a central line load is studied as a specific example. Three different thicknesses to include the range of thin to moderately thick to thick plates are considered and it is shown that by employing a judicious slicing pattern stress variation at the critical sections of the plate can be obtained. Numerical results obtained are compared with those from a thin plate theory and a higher order thick plate theory.

1. INTRODUCTION

It is well known that the photo-elastic method is a powerful experimental tool since it is possible by this method to obtain a complete stress field even for problems with irregular boundaries. A variety of two-dimensional problems has been solved using this technique. However, in practice many stress analysis problems exist which are strictly three-dimensional in character and cannot be effectively approached by employing two dimensional photo-elastic techniques. In recent years many investigators[1-6] have turned their attention to three-dimensional photoelasticity and consequently many methods and materials are available now. However, applications to only few problems exist. Hence the present investigation aims mainly at illustrating the applicability of this method to thick plates. Square plate models of three different thicknesses were cast, machined to final dimensions and stress-frozen. In the example considered, the two opposite edges of the plate are simply supported and the remaining edges are free, the plate being subjected to a central band load. The stress-frozen model is then sliced to remove planes of interest which are then analysed to obtain stress distribution at critical sections. The results obtained from this are compared with those from Reissner and a higher order theory[7].

2. MODEL PREPARATION

Models were cast in galvanised iron moulds. Galvanised iron has been found particularly suited for moulds as castings made in these moulds showed negligible initial stresses due to shrinkage compared to those made out of steel or aluminium mouIds[8]. The materials used are a resin, Araldite CY230, 100 parts by weight and a hardner, pthalic anhlydride, 30 parts by weight. These materials have been used by many investigators and have been found to be ideal for large casting[8, 9].

In order to obtain large castings free of residual stresses, it is almost imperative to prepare the material under closely controlled conditions. The procedure adopted is summarised below.

The resin is first heated to a temperature of about 110^{0}C and has been kept stirring during heating using a mechanical stirrer. The hardner, which is in the form of white flakes is slowly added to the heated resin and the mixture thoroughly mixed, the temperature always being kept between 100^{0}C and 110^{0}C. The resin hardner mixture is properly filtered and transferred into moulds which were priorly coated with a releasing agent and kept at about 95^{0}C in a temperature controlled oven. The temperature is kept constant at 90^{0}C for about 24 hours during which the resin sets and reaches a rubbery state. It is then slowly cooled at the rate of 1^{0}C/hour to room temperature. The moulds are then stripped off and the observed in the polariscope for any possible shrinkage stresses. The models at this ,stage are usually soft and are then subjected to curing cycles by slowly heating up to 110^{0}C and cooling as above. After the models have been significantly hardened they are machined to the required dimensions and stress frozen.

Table 1 gives the model dimensions used and the load applied.

Table 1. Model dimensions and load applied

Model	Dimensions in mm				Concentrated load applied in N
	2a =2b	2h	2c	a/h	
1	200	22.2	25	9	69.22
2	200	33.3	25	6	140.43
3	200	67.0	25	3	229.50

3. STRESS-FREEZING AND CALIBRATION

The model is set up inside the temperature controllable oven. The load is applied by a lever arrangement, top lever ratio of the loading frame used being four. The concentrated load coming from the loading frame will be distributed uniformly over a central band of 25 mm wide. Suitable packing of cork sheet has been placed between the model and the loading block to give a uniform loading. The loading arrangement is schematically shown in fig.1.

The model is heated relatively rapidly to about 120^{0}C and the required load is applied. The temperature is kept fairly constant for about four hours to make it uniform throughout the model. The model is then cooled very slowly at a rate of $\frac{1}{2}^0$ per hour upto about 75^{0}C and then at 1^0 per hour to room temperature. The model is removed and sliced for further analysis.

A circular ring and disc made out of the same material as the model and loaded along the diametral plane has also been placed in the oven along with the model to undergo the same cycle of heating and *coo*ling. Values of E and μ of the material and material fringe value fσ are then calculated from the data obtained from the ring and the disc using the method suggested, by Durelli and Ferrer[10]. The calculated fσ, E and μ values for the three model are given in table 2.

4. ANALYSIS

If the stress pattern frozen into a three-dimensional photoelastic model

Table 2. Material fringe value (fσ), modulus of elasticity (E) and Poisson's ratio (μ)

	fσ		E		μ
Model	Pa-m	psi-in	KPa	Psi	at 120^{0}C
1	332.65	1.90	12479.95	1810	0.45
2	346.66	1.98	13472.83	1954	0.46
3	336.15	1.92	13721.85	1990	0.45

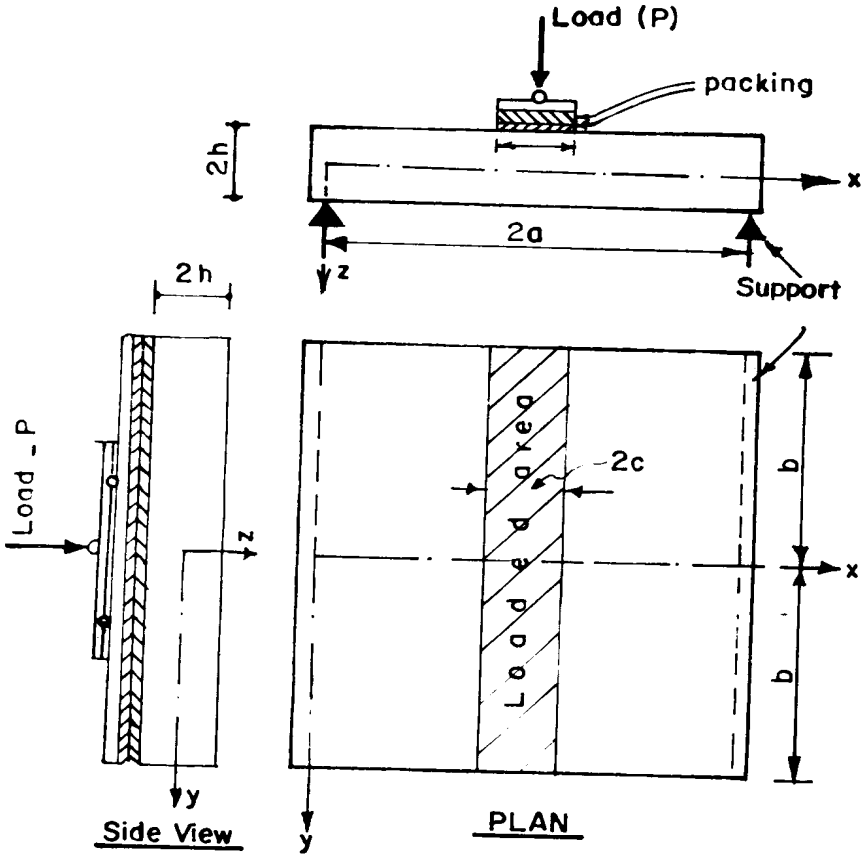

Fig. 1: Co-ordinate directions and loading arrangement

is observed in a polariscope, the resulting fringe pattern cannot, in general be interpreted. The conditioned light passing through the thickness of the model integrates the secondary principal stress difference ($\sigma_1 - \sigma_2$) over the length of the path of the light so that little can be concluded regarding the state of stress at any point.

To circumvent this difficulty the three-dimensional model is sliced to remove planes of interest which are then examined individually to determine the state of stress existing in that particular plane or slice. In studies of this type the slices should be sufficiently thin in relation to the size of the model so that stresses do not change either in magnitude or direction through the thickness of the slice. A slice thickness of 6. 3mm $\left(\frac{1''}{4}\right)$ is used here.

As whole field analysis is not intended only three slices, one along the x-axis called centre slice, a second at the free edge called edge slice (parallel to the x-axis) and a third one at the middle (parallel to the Y-axis) called transverse slice, as shown in fig.2, have been used. Stresses at critical points on the plate are calculated from the data obtained from these slices as follows. Some typical dark and light field isochromatic patterns obtained are shown in fig 3.
It is well-known that when a two-dimensional model is examined in a polariscope the resulting isochromatic fringe pattern can be interpreted to give[9]

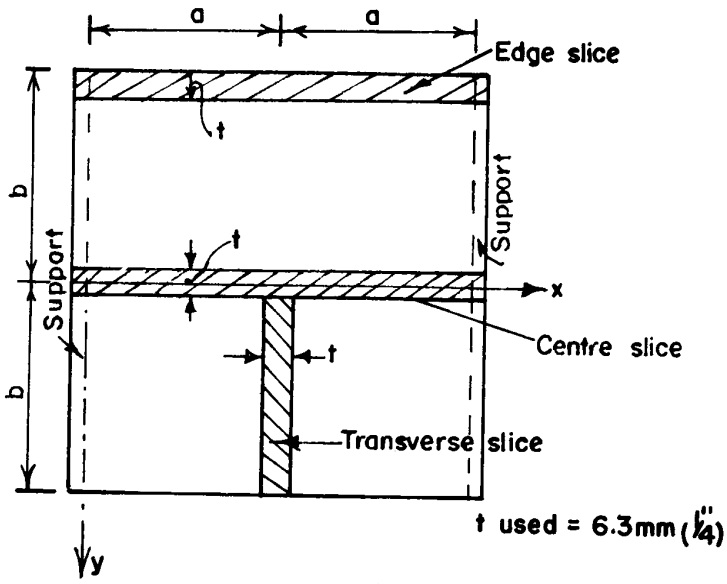

Fig. 2: Plan of the model showing location of different slices.

$\sigma_1 - \sigma_2 = N f_\sigma / t$ ..... (1)

Where $\sigma_1 - \sigma_2$ are principal stresses in the plane of the model, N is the fringe order and t is the thickness of the model.
Thus considering the centre slice which is in the xz plane, the resulting fringe pattern can be interpreted to give

$\sigma_1 - \sigma_2 = N_y f_\sigma / t$ ..... (2)

and because of the symmetry in location of the centre slice, equation (2) for the top and bottom layers namely z = ±h, is written as

$\sigma_x - \sigma_z = N f_\sigma / t$ ..... (3)

σ_z values on z = ±h are known to be equal to the applied load if any. The isochromatic fringe order N_y on z = ±h
are also measured by observing the slice in the polariscope and surface values of σ_x on z = ±h along the centre slice are then calculated using eq.(2) These variations for the three different models are shown in figs. 4(b),5(b) and 6 (b).
The σ_x variations at the top and bottom faces of the free edge can also be determined in a similar manner.
The state of stress at interior points in the model can be determined by using the shear difference method[9] which is based on the numerical integration of the appropriate stress equation of equilibrium. Thus to obtained the variation of transverse normal stress σ_z,, the equilibrium equation in the z direction, namely

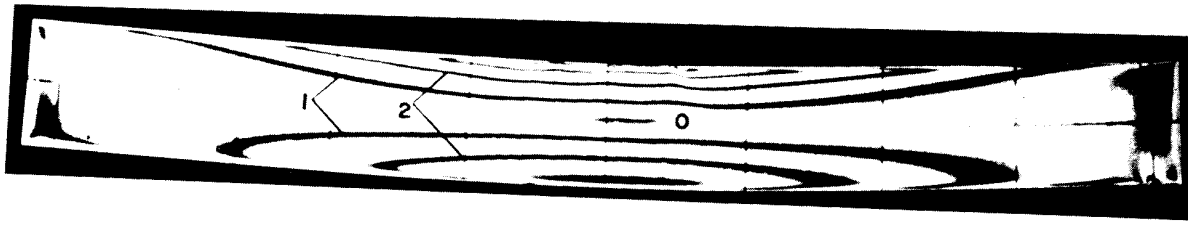

(a) Dark field, centre slice

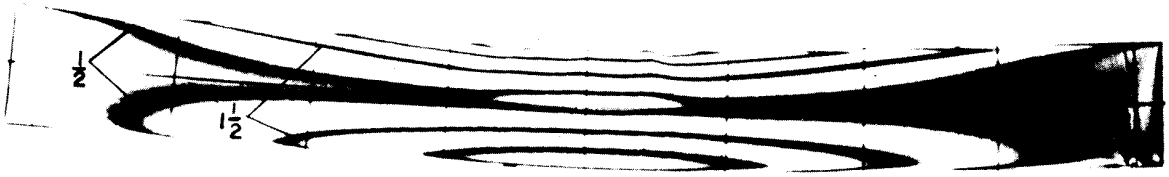

(b) Light field, centre slice

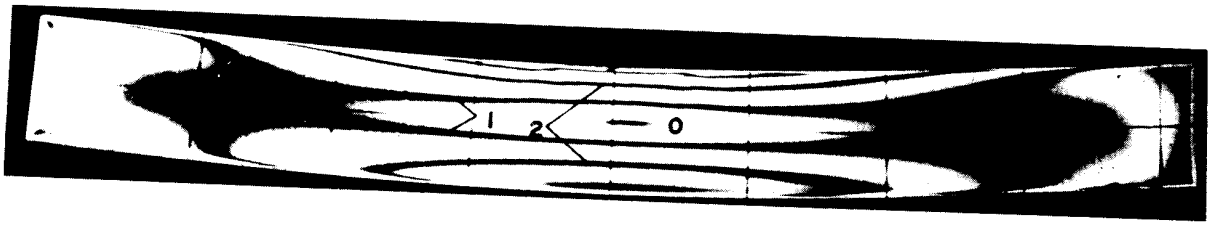

(c) Dark field, edge slice

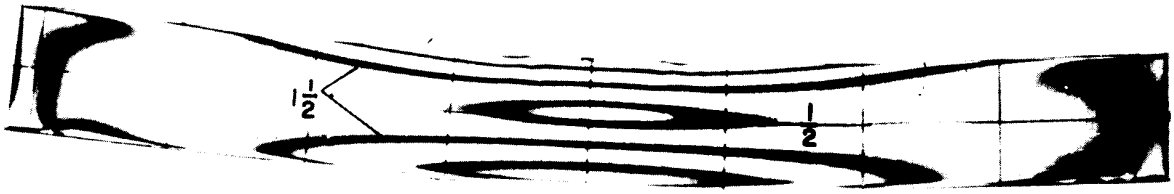

(d) Light field, edge slice

Fig. 3a: Typical isochromatic patterns of centre and edge slices of model no. 1 (a/h = 9)

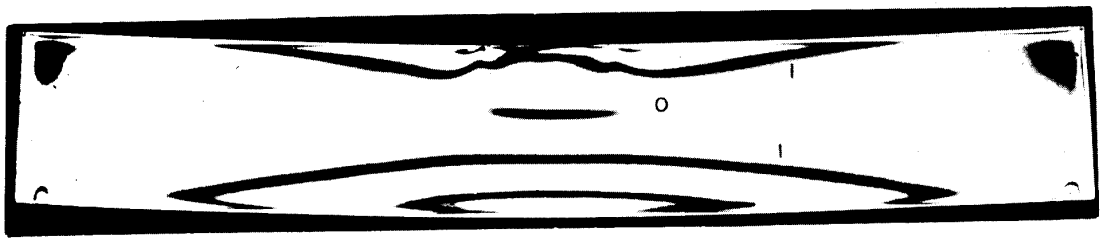

(a) Dark field, centre slice

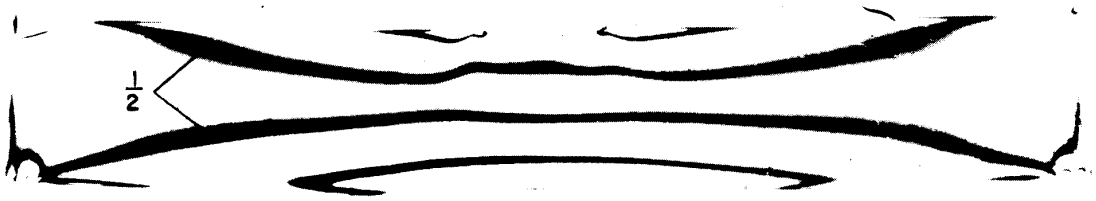

(b) Light field, centre slice

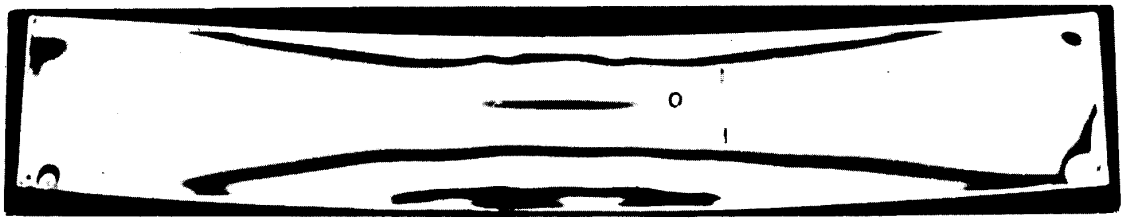

(c) Dark field, edge slice

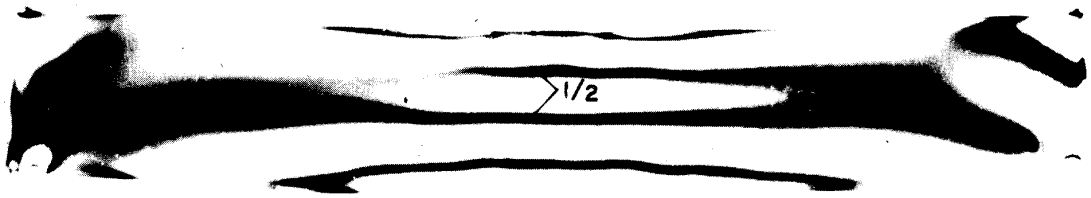

(d) Light field, edge slice

Fig. 3b: Typical isochromatic patterns of centre and edge slices of model no. 2 (a/h = 6)

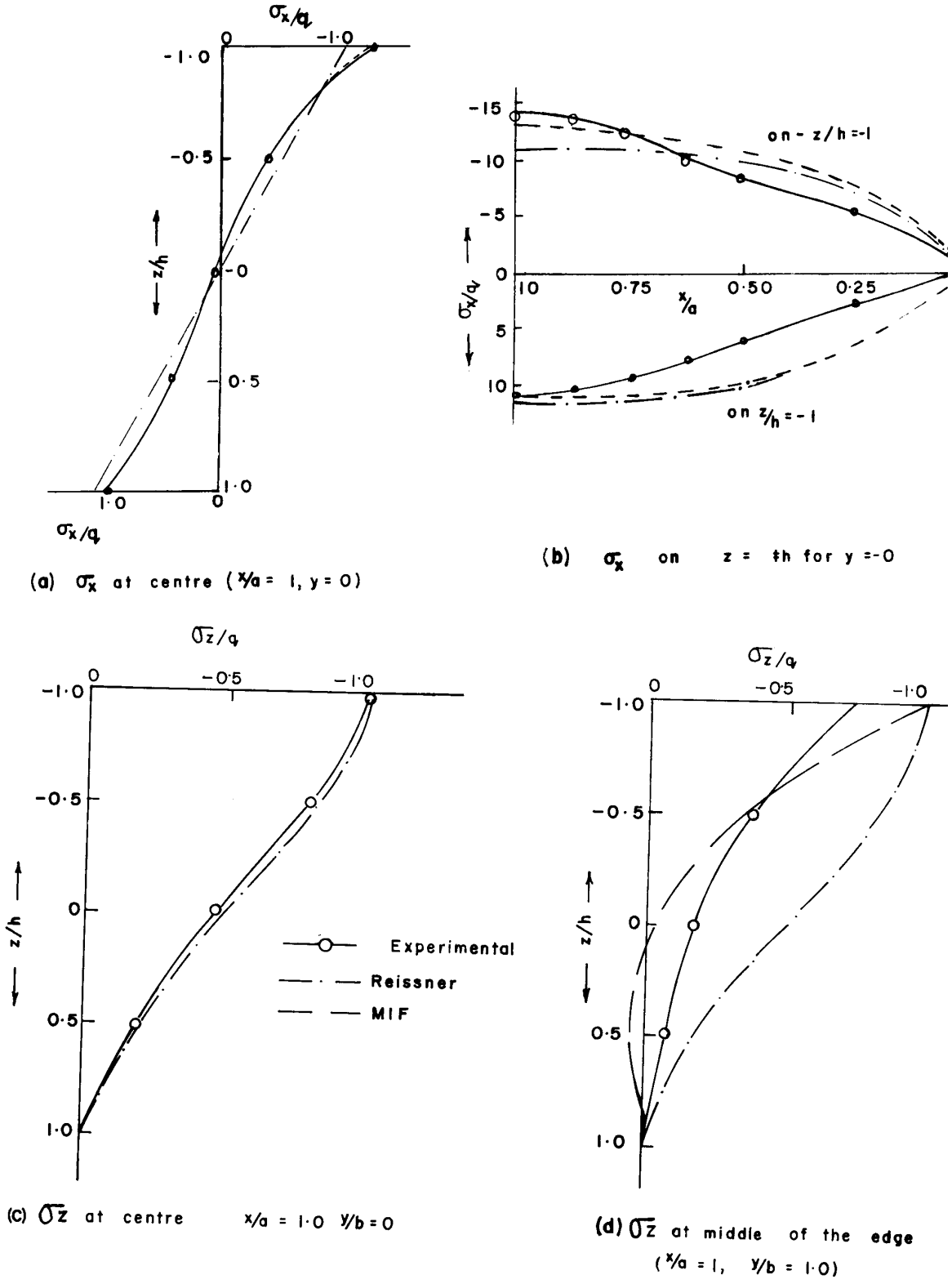

Fig. 4 Variation of √x and √z for the plate with a/h = 9 (model no. 1)

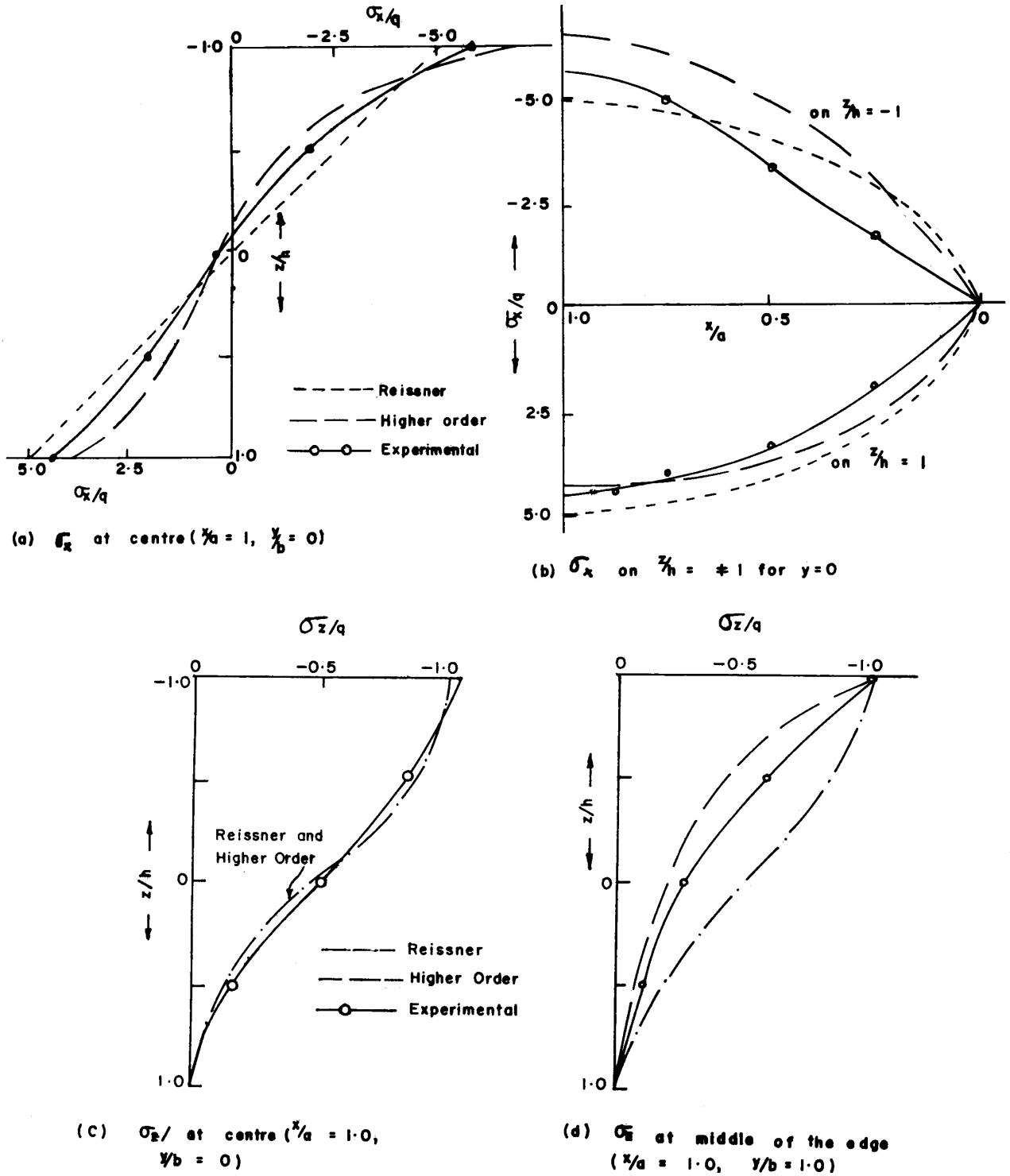

(a) σ_x at centre ($x/a = 1$, $y/b = 0$)

(b) σ_x on $z/h = \pm 1$ for $y = 0$

(C) σ_z at centre ($x/a = 1.0$, $y/b = 0$)

(d) σ_z at middle of the edge ($x/a = 1.0$, $y/b = 1.0$)

Fig5 Variation of √x and √z for the plate with a/h = 6 (model no.2)

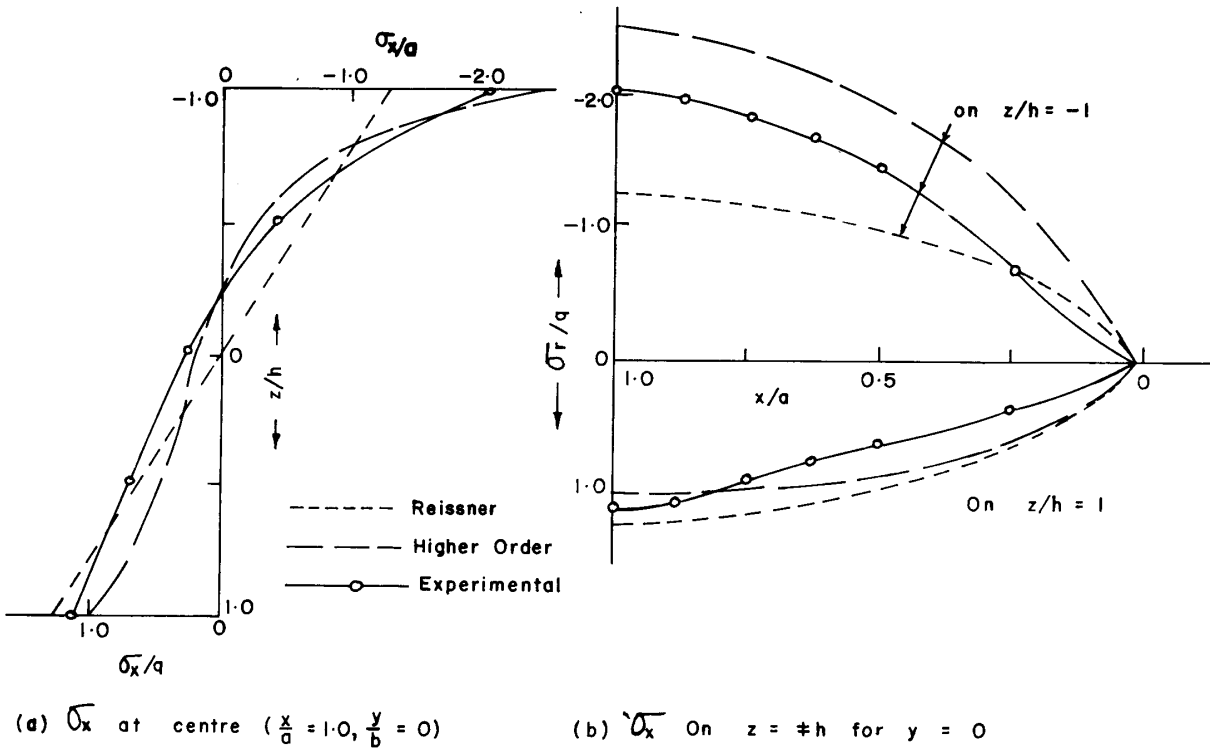

(a) σ_x at centre ($\frac{x}{a}$ = 1·0, $\frac{y}{b}$ = 0) (b) σ_x On z = ±h for y = 0

Fig. 6 Variation of √x and √z for the plate with a/h = 3 (model no.3)

$$\frac{\delta\tau_{xz}}{\delta_x}+\frac{\delta\tau_{yz}}{\delta_y}+\frac{\delta_{\sigma z}}{\delta_z}=o \quad \text{.....(4)}$$

is numerically integrated and which when written in th finite difference form is:

$$\sigma_z\Big|_{z_1}=\sigma_z\Big|_{z_o}-\frac{\Delta\tau_{xz}}{\Delta_x}\Delta_z\Big|_{zo}^{z1}-\frac{\Delta\tau_{yz}}{\Delta y}\Big|_{zo}^{z1} \quad \text{..... (5)}$$

When $\Delta_x = \Delta_z$ equation (5)

$$\sigma_z\Big|_{z_1}=\sigma_z\Big|_{z_o}-\Delta\tau_{xz}\Big|\frac{zo+z1}{2}-\Delta\tau_{xz}\Big|\frac{zo+z1}{2} \quad \text{..... (6)}$$

By continuing this integration in a stepwise procedure it is possible to write

$$\sigma_z\Big|_{z_2}=\sigma_z\Big|_{z_1}-\Delta\tau_{xz}\Big|\frac{z_1+z_2}{2}-\Delta\tau_{xz}\Big|\frac{z_1+z_2}{2} \quad \text{..... (7)}$$

sAnd so on whch for any $_z\lambda$can be written as

$$(\sigma_z)\lambda=(\sigma_z)o-\sum_o^{\lambda}\Delta\tau_{yz} \quad (8)$$

The shear stresses τ_{xz} and τ_{yz} are calculated using

$$\tau_{xz} = \frac{N_y f_\sigma}{2t} \sin 2\theta_y \quad \text{.....(9)}$$

$$\tau_{yz} = \frac{N_x f_\sigma}{2t} \sin 2\theta_x \quad \text{.....(10)}$$

where the fringe orders N_x and N_y are obtained from transverse and centre slices respectively. Having obtained the shear stress differences $\Delta\tau_{xz}$ and $\Delta\tau_{yz}$ at various points from the above, the integration represented in eq. (8) is carried out from a point where $(\sigma_z)_o$ is known, in this problem the bottom of the plate where σ_z = o. The σ_z variations so calculated at the centre of the plate are shown in fig. 4(c) and 5(c) for models 1 and 2 respectively. Similar analysis performed for the centre of the edge slice yielded σ_z variations as shown in figs. 4(d) and 5(d).

Variation of normal stress at centre across the thickness is σ_x obtained from the equation[9].

$\sigma_x = \sigma_z - (\sigma'_1 - \sigma'_2) \cos 2\theta_y$

$$\sigma_z - \frac{N_y f_\sigma}{t} \text{Cos } 2\theta_y \quad \text{.....(11)}$$

and the results for the three models are presented in figs. 4(a) , 5(a) and 6(a) respectively.

5 ·NUMERICAL RESULTS AND DISCUSSION

From the dimensions of the model shown in table 1 it can be seen that the thicknesses were so chosen to include examples on a thin (a/h = 9),a moderately thick (a/h = 6) and a thick (a/h = 3) plate. It has been found that the load applied should be sufficiently large to produce enough number of fringes lest the accuracy of the results will be considerably affected. It was noticed that the load applied for models 2 and 3 should have been higher. In figs. 4 ,5 and 6 in addition to the present experimental results, those obtained from a 14th Order MIF theory 7 and Reissner or classical theory results are also shown for comparison.

In figs. 2 and 3 it can be seen that the isochromatic patterns for the centre and edge slices are nearly identical which can be expected as the plate is in cylindrical bending. The σ_x variation predicted by experiment agrees very well with the higher order theory especially near the centre of the plate (figs. 4a, 5a and 6a). The deviation between the two near the supports (figs. 4b, 5b and 6b) may be due to the difference in edge conditions; the plate in the photoelastic experiment was supported on knife edges while In the theoretical analysis a 'friction clamped' edge defined by boundary conditions w = σ_x = v = o has been used. Transverse normal stress, Oz obtained from experiment compares very well with MIF theory (igs. 4c, 4d, 5c and 5d) and it can be seen that Reissner theory prediction of σ_z at the free edge is quite different from the actual distribution but agrees very well at the centre.

6. CONCLUSION

A method for investigating thick plates using the stress freezing technique of three dimensional photo-elasticity and the shear difference method, has been presented. The applicability of this method has been illustrated by considering three rectangular plate models and it has been shown that by employing a judicious slicing pattern stresses at critical sections of the plate can be determined with the help of few slices Comparison of experimental result with those obtained from theory leads

to the conclusion that sufficiently accurate result can be obtained by this method. The experimental procedure presented will be quite useful in determination of stresses in thick plates of irregular shapes and subjected to non-typical loading for which theoretical solutions rarely exist.

ACKNOWLEDEMENT

The experimental part of the work reported in this paper was carried out by the author at the Department of Civil Engineering, Indian Institute of Science, India. The author sincerely acknowledges the help and suggestions received from Professors K. Chandrashekhara and K.T.S. Iyengar, during the course of the above investigation.

REFERENCES

1. Hetenyi, M. The fundamentals of three-dimensional photoelasticity, J. Appl. Mech., Vol. 5., 1938, pp 149-155

2 Hetenyi, M. The application of the hardening resin in three-dimensional photoelastic studies, J. Appl. Phys., Vol. 10, 1938, pp. 295-300.

3. Durelli , A.J. and R.L. Lake, Some unorthodox procedures in photoelasticity, proc, SESA, Vol. IX 1951, pp 97-122

4. Dally, J.W., A.J. Durelle and W.F. Riley, A. new method to lock-in elastic effects for experimental strees analysis, J. Appl. Mech. Vol. 25, 1958 pp. 189-195.

5. Frocht. M.N. and Pih. H., A new cornmentable material for two and three dimensional photoelastic research, Proc. SESA Vol.XII, 1954. pp 55-64.

6. Leven, M.M., Epoxy resins for photoelastic use in photoelasticity, Pergarnm press, Now York, 1963.

7. Iyengar K.T.S., Chandrashekhara, K and Sebastian, V.K., on the analysis thick rectangular plates, Igenieur - Archiv, Vol. 43, 1974, pp 317-330.

8. Chandrashekhara, K, Abraham Jacob, K, and Iyengar, K.T.S. Three-dimensional photoelastic analysis of anchorage zone stresses in post-tensioned concrete members, CBIP report, Dept. of Civil Engineering Indian I Institute of Science, Bangalore, 1974.

9. Dally, J. W. and Riley, W. F ., Experimental stress analysis McGraw-Hill Book Co., New York, 1965, pp. 252-279.

10 Durelli, A.J. and Ferrer, L. New methods to determine elastic constants, Materials and standards; Vol. 3, 1963, pp 988-991.